

CHAPTER 154

A model for cross shore sediment transport

Irene Katopodi and Nikos Kitou¹

Abstract

In this paper a mathematical model for the computation of the cross shore sediment transport for random waves is presented. The model consists of the hydrodynamic, the suspended sediment transport and bed load modules. The suspended sediment concentration is computed with the use of the wave-averaged convection diffusion equation. The vertical structure of both the wave-induced current and suspended sediment concentration are modelled with the use of quasi-3d techniques. Mechanisms for the offshore transport (undertow) and the onshore transport (Lagrangian transport, transport due to wave asymmetry) are included. The model is tested against an experiment with random waves at prototype scale.

Introduction

The computation of the sediment transport, being an essential element in the understanding and ultimately the control of the morphological processes is a subject that has received a lot of attention in the last decades. Still, the complexity of the various phenomena has not allowed for predictions accurate enough for the design and maintenance of coastal works. This is one reason for the wide variety of existing mathematical models (for a review, see Roelvink and Brøker, 1993).

In the present model the hydrodynamic and the sediment transport parts are an extension of the work of Katopodi et al (1992) where the wave driven current and the suspended sediment concentration were computed with quasi-3D analytical/numerical methods. Thus the vertical distributions of the velocity and concentration were retained at a computer cost almost similar to that of depth-averaged models. Moreover, with the use of the convection-diffusion equation the horizontal variation of the concentration was resolved, a factor that it is believed to have an important impact to the bed level changes (see Katopodi and Ribberink, 1992). The model is extended for random waves and the Lagrangian drift is incorporated to account for the wave transport.

For the bed load two alternatives based on the formula of van Rijn (1985) were tried, a wave averaged and an interperiod formulation. The latter can take into account the wave asymmetry. The bed slope effect is included in both formulations.

1. Democritus Univ. of Thrace, Dept. of Civil Eng., 67100 Xanthi, Greece

Moreover, wave heights, set-up, wave-mean velocities and (total) sediment transport are compared with experimental data from the Delta Flume experiment (S.-Arcilla et al, 1994) conducted in prototype conditions.

Hydrodynamics

The wave heights are computed from of the wave energy equation.

$$\frac{\partial E_f}{\partial x} = - D_b - D_f \quad (1)$$

where: E_f , D_f , and D_b are the energy flux, the dissipation due to bottom friction and the dissipation due to breaking.

Battjes and Janssen (1978) proposed a formulation for D_b proportional to the fraction of breaking waves Q_b . They also derived the fraction of breaking waves from a simple parameterization of the breaking wave height distribution from a Rayleigh distribution.

The current velocities are computed using the quasi-3D model of de Vriend and Stive, (1987) as modified by Ribberink and de Vriend (1989) to take into account the wave boundary layer effects. This model is based on a profile function technique combined with a 2DH current formulation. The current is divided into a primary component and a number of secondary components due to the vertical nonuniformities of the various driving forces. The effects of wave breaking, bottom dissipation and boundary layer streaming are included. The velocity profile is given as a sum of components due to the various driving forces:

$$U(\zeta) = U_1(\zeta) + U_2(\zeta) + U_3(\zeta) + U_4(\zeta) + U_5(\zeta) \quad (2)$$

where $U_1(\zeta)$, $U_2(\zeta)$, $U_3(\zeta)$, $U_4(\zeta)$ and $U_5(\zeta)$ are the primary current, the secondary current due to surface shear stress, the secondary current due to secondary bottom shear stress, the near-bottom drift due to spatial variation of the orbital velocity and the near-bottom drift due to the boundary layer respectively.

The wave and the current model were tested against the Delta Flume'93 experiment (see S.-Arcilla et al., 1994) conducted in the Delta Flume of Delft Hydraulics. The flume dimensions are length 225m, width 5m and depth 7m. The experiment included tests with two geometries, i.e. equilibrium parabolic Dean-type profile with and without a dune, and three "dynamic states", i.e. near-equilibrium, erosive and accretive conditions. The hydrodynamic model is tested against test 1A (profile without a dune, near equilibrium conditions). Narrow banded random waves were used and the wave characteristics were $T=4.83$ s and $H_{rms} = 0.62$ m. The D_{50} of the sand was 0.2 mm. The bed configuration after two hours of wave action is used for the calculations, see Fig. (2). The bed roughness is taken 1cm.

In Fig. (1a) the root-mean-square wave height computed with the model is shown together with measurements conducted with wave height meters. We can see that the overall agreement is rather good.

In Fig. (1b) the computed fraction of breaking waves is presented. Two major peaks can be seen before and after 150m. A third extreme peak appears near the shoreline ($Q_b=1$). As explained by Battjes and Janssen (1978) the wave model is not valid in this region but the solution in the rest of the domain is not contaminated. Nevertheless, the unnatural

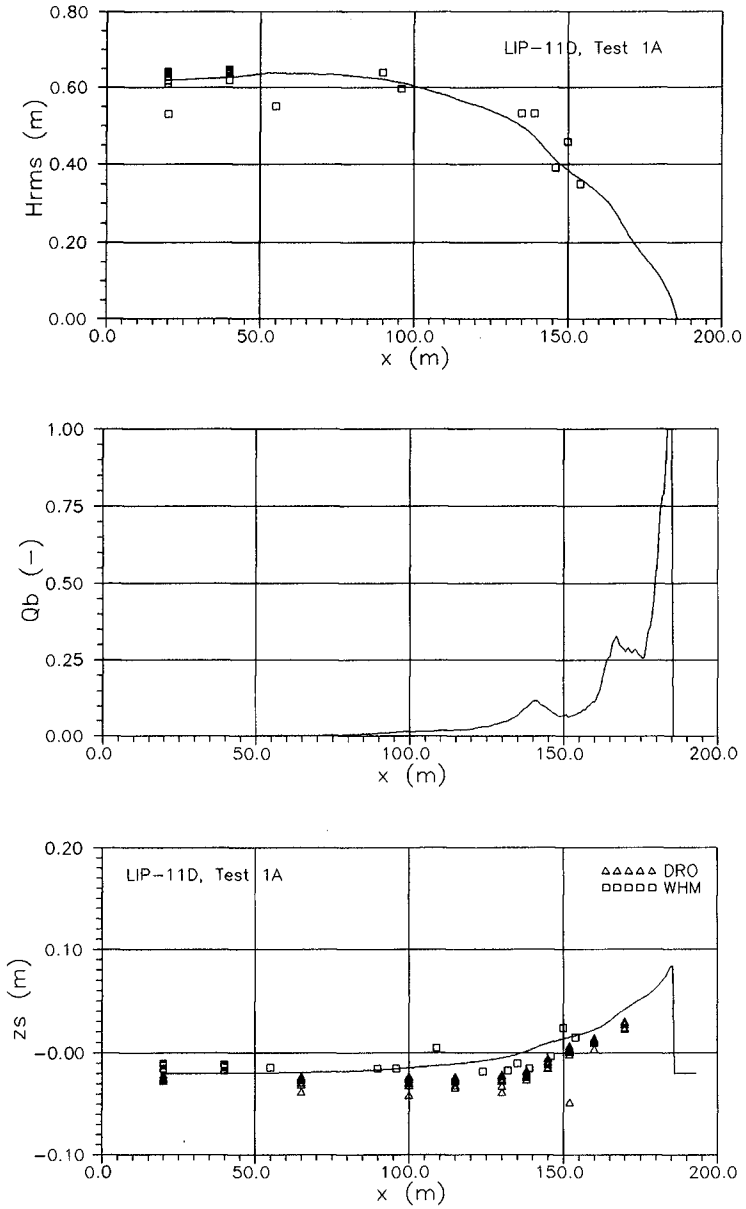


Fig.1 a) Wave height, b) Fraction of breaking waves, c) Set-up

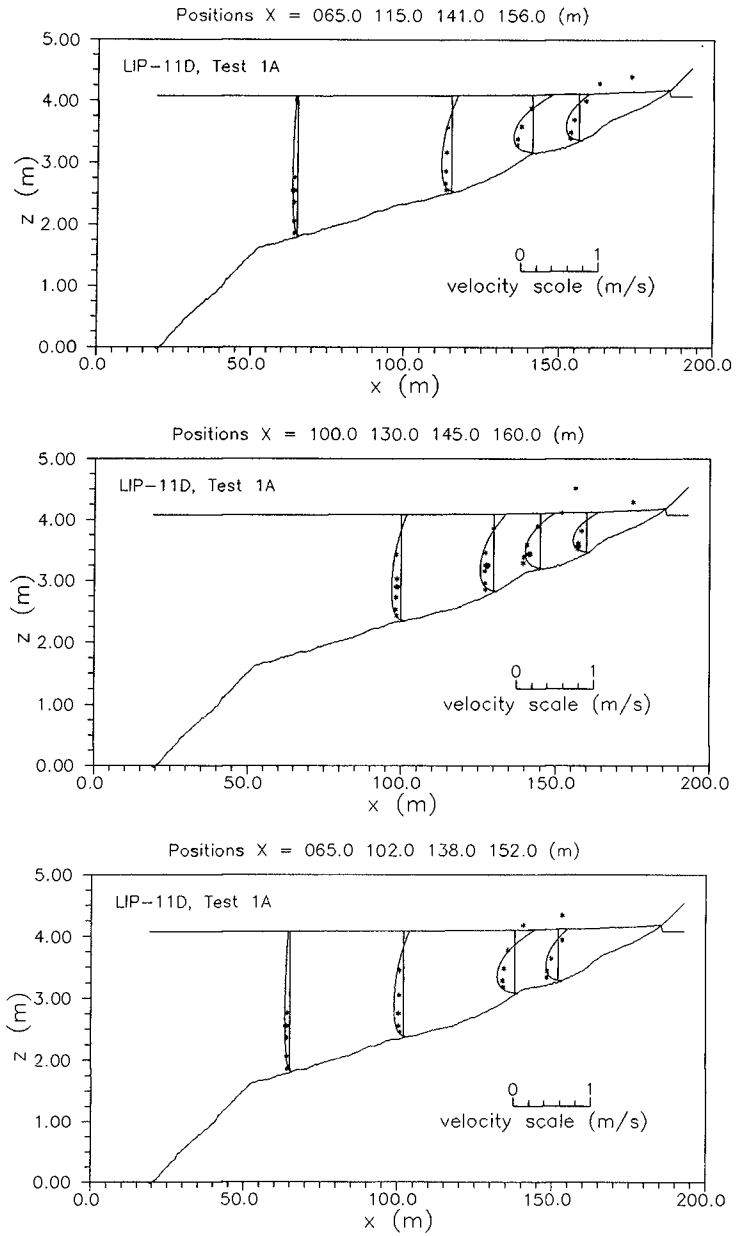


Fig.2 Velocity profiles

behaviour of Q_b close to the shoreline has a local impact in all the quantities that are computed in the following (e.g. set-up, bed shear stress, undertow, suspended sediment transport, bed load).

In Fig. (1c) the computed set-up is depicted together with measurements from wave height meters (WHM) and pressure sensors (DRO). The latter are considered more accurate (S.-Arcilla et al, 1994). We can see that the set-up is somewhat overpredicted by the model, owing to the formulation of the driving forces in the depth averaged momentum equation (set-down was excluded, see de Vriend and Stive, 1987).

In Fig. (2) the computed horizontal velocity profiles are shown together with the measurements conducted with two component electromagnetic flow meters in several cross sections. The model overpredicts the velocities in all cross-sections. In the main body of the water (under the wave trough) the curvature of the computed profiles is larger than in measurements that tend to have a more uniform profile over the depth. Yet the results are encouraging once certain aspects of the hydrodynamic model can still be improved. Of course the measurements between trough and crest should not be compared with the model due to the partial presence of the water at the sensors during the wave cycle.

Sediment transport

The total sediment transport is the sum of the suspended sediment and the bed load transport. The suspended sediment transport is computed with the model of Katopodi et al. (1992) where the wave-induced transport caused by the Lagrangian velocity is added. The bed load is modelled with a) the formula of van Rijn (1985) derived for wave averaged transport and b) the same formula applied here for instantaneous transport during the wave cycle. In principle, the instantaneous (or interperiod) formula can take into account the wave asymmetry.

Suspended sediment transport.

The suspended sediment is computed in terms of the suspended concentration and of the velocity. For the suspended sediment concentration the model of Katopodi and al (1992) is used (see also Katopodi and Ribberink, 1992). This model is based on an asymptotic solution (Galappatti and Vreugdenhil, 1985) of the wave averaged 3D convection diffusion equation. The model uses the mixing coefficient and the near-bed reference concentration of van Rijn (1986).

The depth averaged convection diffusion equation (Katopodi et al, 1992), reads:

$$\bar{c}_e = (1 + V_T + V_X)\bar{c} + T_A \frac{\partial \bar{c}}{\partial t} + L_X \frac{\partial \bar{c}}{\partial x} - T_A \frac{\partial}{\partial x} \left(\epsilon_x \frac{\partial \bar{c}}{\partial x} \right) \quad (3)$$

with

$$T_A = \frac{\gamma_{21}}{\gamma_{11}} \frac{h}{w_s}, \quad L_X = \left(\sum_{i=1}^n \bar{U}_i \frac{\gamma_{22,i}}{\gamma_{11}} \right) \frac{h}{w_s} \quad (4)$$

$$V_T = \left(\beta \frac{\gamma_{23}}{\gamma_{11}} + \frac{\gamma_{24}}{\gamma_{11}} \right) \frac{1}{1+\beta} \frac{\partial z_s}{\partial t} \frac{1}{w_s} \quad (5)$$

$$V_x = \sum_{i=1}^n \left(\frac{\partial}{\partial x} (\bar{U}_i h) \frac{\gamma_{25,i}}{\gamma_{11}} \right) \frac{1}{w_s} \quad (6)$$

where \bar{c} and \bar{c}_e are the depth averaged and the equilibrium concentration, \bar{U}_i the depth averaged horizontal velocities, and w_s the sediment fall velocity. The coefficients γ_{ij} depend only on the explicit knowledge of the vertical mixing coefficient, the fall velocity and the normalized velocity profiles and are computed before the solution of (3). The coefficient β is the reference level normalized by the depth h . The index i denotes the number of similarity profiles that constitute the undertow velocity ($i=1-5$) and the Lagrangian drift ($i=6$).

Equation (3) describes the adjustment of the depth averaged concentration to its equilibrium value. The parameters TA and LX are characteristic scales in time and space of this adjustment process (adaptation time, adaptation length). The terms VT and VX arise from the vertical coordinate transformation and from the inclusion of the vertical velocities that are computed via the continuity equation, respectively.

The above equation has been derived for "concentration" bed boundary condition (the concentration at the reference level is assumed to adapt immediately to equilibrium conditions). A similar equation holds for "gradient" bed boundary condition (the near-bed vertical gradient of the concentration adapts immediately to equilibrium conditions).

The suspended sediment transport, equation (7), actually is computed in terms of the depth averaged velocity (undertow plus Lagrangian) and concentration and of already computed coefficients (cf Katopodi and Ribberink, 1992).

$$S_x = h \int_0^1 U c \, d\zeta - h \int_0^1 \epsilon_x \frac{\partial c}{\partial x} \, d\zeta \quad (7)$$

After equation (3) has been solved for \bar{c} , the vertical concentration profile, if desired, can be constructed in terms of already known profile functions (see Katopodi and Ribberink, 1992).

The effect of the Lagrangian velocity on the sediment particles is incorporated in the model to account for the wave induced transport. In progressive waves there is a net forward motion of the water particles related to the mass carried forward by the wave crests plus the mass deficiency carried backwards by the troughs (Longuet-Higgins, 1969). As a consequence there is also a net forward sediment transport over the wave cycle. In the computation of the concentration the Lagrangian velocity profile is incorporated as a sixth profile:

$$U_L(z) = \omega k \frac{H^2}{8} \frac{\cosh 2k(z+h)}{\sinh^2 kh} \quad (8)$$

where ω is the wave angular frequency, k the wave number, H the wave height, h the water depth and z the vertical coordinate positive upwards the mean water level.

The integral of the above expression (8) over the depth yields the wave mass flux. Although the undertow profile and the Lagrangian profile are in volumetric balance for a steady state cross-shore case, the

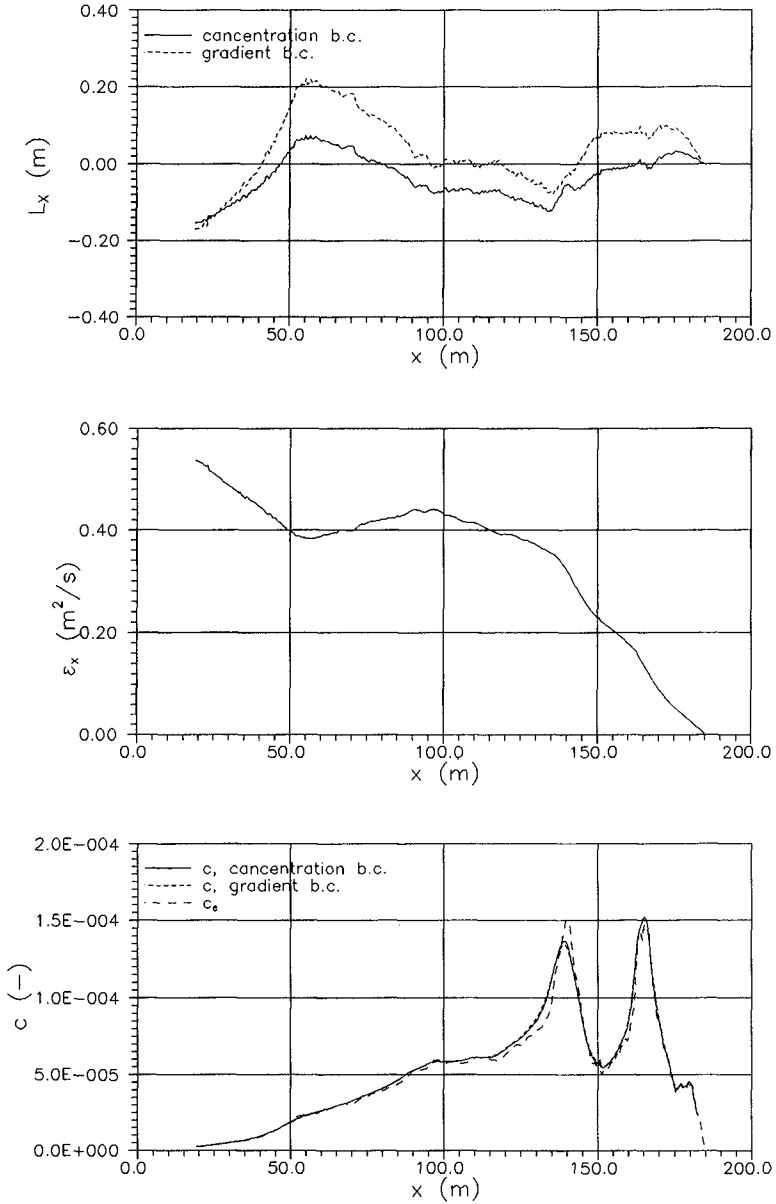


Fig.3 a) Adaptation length, b) horizontal eddy viscosity
c) Depth-averaged concentration

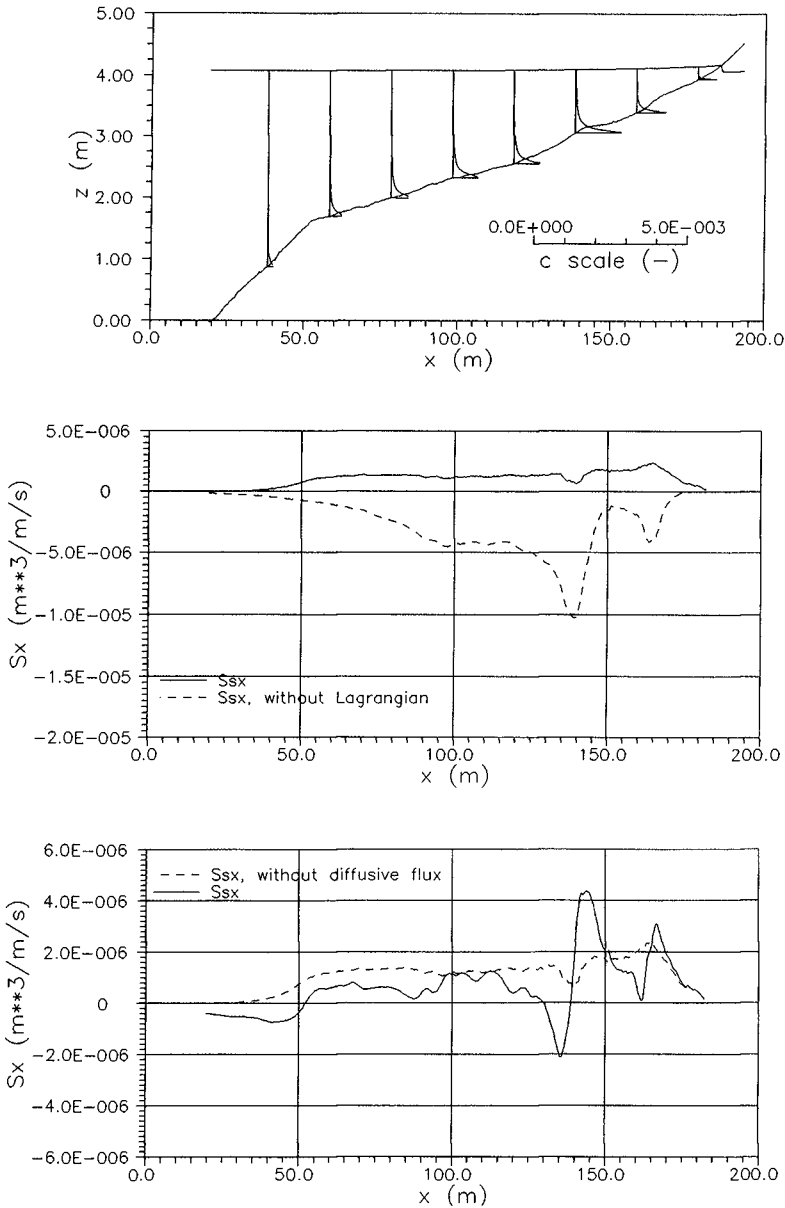


Fig.4 a) Concentration profiles along the flume.
 b) Suspended sediment transport (with and without Lagrangian),
 c) Suspended sediment transport (with and without diffusive part)

resultant sediment transport is not. The sign and the magnitude of the suspended sediment transport depends on the local profile shapes of undertow, Lagrangian drift and concentration.

In Fig. (3a) the adaptation length along the flume is shown for concentration and for gradient bed boundary conditions. The magnitude of the adaptation length is smaller than the space step (0.5m) and as a result the concentration is expected to be close to equilibrium (cf Katopodi and Ribberink, 1992). In Fig. (3b) the horizontal eddy viscosity for the computation of the concentration is shown (Katopodi et al, 1992).

Fig. (3c) presents the depth averaged non-equilibrium concentration for the two bed boundary conditions as well as the equilibrium concentration. Very small differences exist between the equilibrium and the non-equilibrium concentrations, as expected from the magnitude of the adaptation length. Clearly, the concentration adapts immediately to local conditions. The concentration presents two major peaks and a smaller spurious peak near the shore line.

In Fig. (4a) the profiles of the concentration are shown at various cross-sections along the flume. Not much concentration is in suspension and most of it is concentrated near the bottom.

In Fig. (4b) the suspended sediment transports computed with only the wave mean velocity and with the inclusion of the Lagrangian velocity are presented. It is clear that the Lagrangian transport is in the onshore direction and has such a strong influence on the transport that it reverses the sign of the wave mean transport everywhere in the flume.

Fig. (4c) depicts the suspended sediment transport computed with only the first term (convective transport) of equation (7) and with the second term (diffusive transport) also included. The impact of the diffusive transport is strong especially in zones with large horizontal gradients of the concentration (e.g. see the concentration peaks in Fig. 3c).

Bed Load

For the computation of the bed load two formulations have been tried. One wave averaged and one interperiod. For the wave averaged formulation the formula of van Rijn (1985) was used:

$$\dot{S}_b = (\Delta g D_{50}^3)^{1/2} 0.053 \frac{1}{D_*^{0.3}} T^{2.1} \text{sign}(\bar{\tau}_{cw}) \quad (9)$$

where

$$T = (|\bar{\tau}_{cw}| - \tau_{cr}) / \tau_{cr} \geq 0, \quad \bar{\tau}_{cw} = \mu_c \bar{\tau}_c + \mu_w \bar{\tau}_w$$

with $\bar{\tau}_{cw}$ the combined bed shear stress for currents and waves as function of $\bar{\tau}_c$, $\bar{\tau}_w$ the current related and wave related bed shear stress respectively. The critical shear stress for the initiation of motion (Shields) is denoted by τ_{cr} . D_* is the dimensionless particle parameter which is function of the median particle diameter D_{50} , Δ is the relative apparent density of the bed material and g the acceleration of gravity.

The formula of van Rijn involves the significant wave height in the calculation of the orbital velocity. In our model H_s is computed as a function of H_{rms} and Q_b .

In the above formulation the waves are used as a stirring mechanism while the current transports the sediment. The formula was chosen because

it contains the same parameters as the reference concentration we used for the suspended sediment part and because it has well proved its validity for unidirectional flows. Of course wave asymmetry can not be implemented.

In asymmetric waves during a short fraction of the wave cycle, strong forward velocities occur transporting big amounts of sediment while during a longer fraction weak backward velocities transport small amounts of sediment. Over the whole wave cycle there is a net forward transport. For short waves (high frequencies) it can be assumed that the asymmetry effect on the sediment transport is concentrated close to the bottom (no time for the concentration to fill the water column) and as such it can be incorporated in the bed load only. For longer waves (low frequencies) the asymmetry transport should be considered for the whole depth. Near the shore the waves are asymmetric.

In order to be able to account for interperiod effects such as the wave asymmetry, following an idea of Ribberink and de Vriend (1989), the same formula (van Rijn) was also used in interperiod mode for the calculation of the instantaneous transport. The only difference now is that the wave related shear stress and consequently the dimensionless shear stress parameter T as well as the transport are functions of time and vary during the wave cycle. The bed load transport is computed by numerical integration of the instantaneous transport over the wave period.

It is understood that the formula of van Rijn has been calibrated to compute convective wave averaged transport but the use of unidirectional flow formulae for instantaneous transport has been suggested and verified before (see Ribberink and de Vriend, 1989). An additional advantage of the formula of van Rijn is that it is provided with a threshold of motion.

At first the interperiod formula was used for sinusoidal waves to check the tendencies of the bed load transport in relation to the wave averaged formula and the order of magnitude of the transport. Then, a form of asymmetry was added by using non-linear second order Stokes waves.

$$U_{orb}(t) = U_1 \cos(\omega t) + U_2 \cos(2\omega t) \quad (10)$$

In order to avoid a secondary maximum in the trough of the orbital velocity the second harmonic was bounded by the relation $U_2 \leq U_1/5$.

Another element taken into account in the bed load formulation is the bed slope effect. This mechanism which is present in nature plays an important role in the morphodynamic computations because it stabilizes the solution by giving the computed bed slope the natural limit of the slope of the bed material internal friction.

In the formulation chosen (see e.g. Fredsøe and Deigaard, 1992) the critical bed shear stress is scaled by a factor α_s that takes into account the relation of the bed slope to the slope of the internal friction.

$$\alpha_s = \frac{\tan \phi}{\cos \beta (\tan \phi \pm \tan \beta)} \quad (11)$$

where ϕ is the angle of internal friction, property of the bed material and β is the local bed slope. The sign (+) holds for downsloping motion of the water while the sign (-) holds for upsloping motion. In our computations the critical shear stress was taken 0.18 N/m^2 and $\phi = 25$ degrees (sand with small amount of organic material).

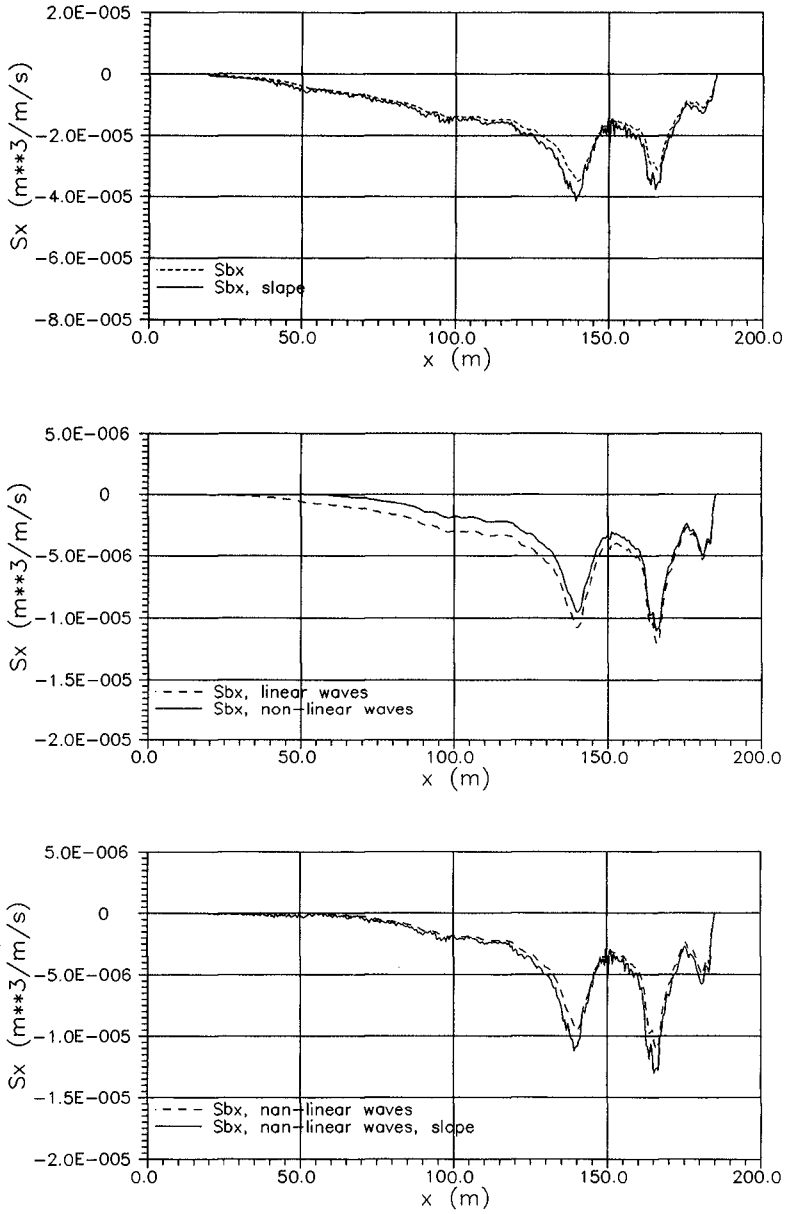


Fig.5 a) Bed load with and without slope effect (wave-averaged formula),
 b) Bed load (interperiod formula with sin and Stokes waves),
 c) Bed load with and without slope effect (Stokes waves)

Although the above formula has a clear meaning in instantaneous mode, it was used also for the wave-averaged formulation once the formula is equipped with the threshold of motion in the parameter T .

In Fig. (5a) the bed load transport computed with the wave-averaged formula with and without the bed slope effect is shown. Fig. (5b) presents the interperiod bed load transport computed with sinusoidal and with Stokes waves. Fig. (5c) shows the slope effect on the bed load for Stokes waves. The magnitude of the transport in the interperiod formulations is smaller than that of the wave averaged one. The tendencies though are similar as well as the positions of the bed load maxima. It looks encouraging to calibrate the formula for instantaneous use. For Stokes waves the effect of the wave asymmetry is clear compared with sin waves, especially in the offshore region where we have some onshore transport. In general, the presence of the wave asymmetry tends to add onshore transport. The bed load including the slope effect has a noisy shape but it looks that exactly this immediate reaction to the bed slope is needed for the correct computation of the bed level changes.

Total load

The total load is the sum of the suspended and the bed load. The total transport is presented for the wave averaged (Fig. 6a) and for the non-linear interperiod bed load formulation (Fig. 6b). We can see that the suspended transport is a small fraction of the total transport, something expected from the computation of the concentration once there is not much sand in suspension. In the interperiod formulation the suspended transport moves the main peak somewhat offshore and results in onshore transport from 50 to 70 m.

In Fig. (7a) the total transport computed with the wave averaged and the interperiod non-linear formulation is shown.

Fig. (7b) shows the measured (total) transport as derived from the measured bed levels at different times of the experiment. The transport estimated from the bed level changes between 02-07, 07-12 and 02-12 hours of the experiment is shown.

As previously mentioned, test 1A was designed to be near equilibrium and it was successful at that. The max difference in bed level between hours 02 and 12 (wave action of 10 hours) was 15 cm locally at the main bar while in most of the flume it was of the order of 1-2 cm. Such small changes would not have an important impact on the hydrodynamic and the sediment transport computations. Thus, although in our model we used the bed configuration after 02 wave hours in the experiment, the computed quantities were compared with all data regardless of the time taken. The transport estimated by such small differences contains large uncertainties. This is why we included in Fig. (7b) all three curves.

The averaged formulation seems to underpredict the transport in the deepest part of the flume (from 0 to 80m) and to overpredict (factor of 2) the transport in the region before breaking (say from 80 to 155m). The peak at 165 m is reproduced at the correct location and agrees rather well in magnitude. The peak at 145 m is shifted about 7 m offshore and its magnitude is clearly overpredicted. The small peak near the shore owes its presence to the unrealistic values of Q_b .

The interperiod model clearly underpredicts the transport. Again the two peaks in the surf zone are reproduced and the overall shape of the

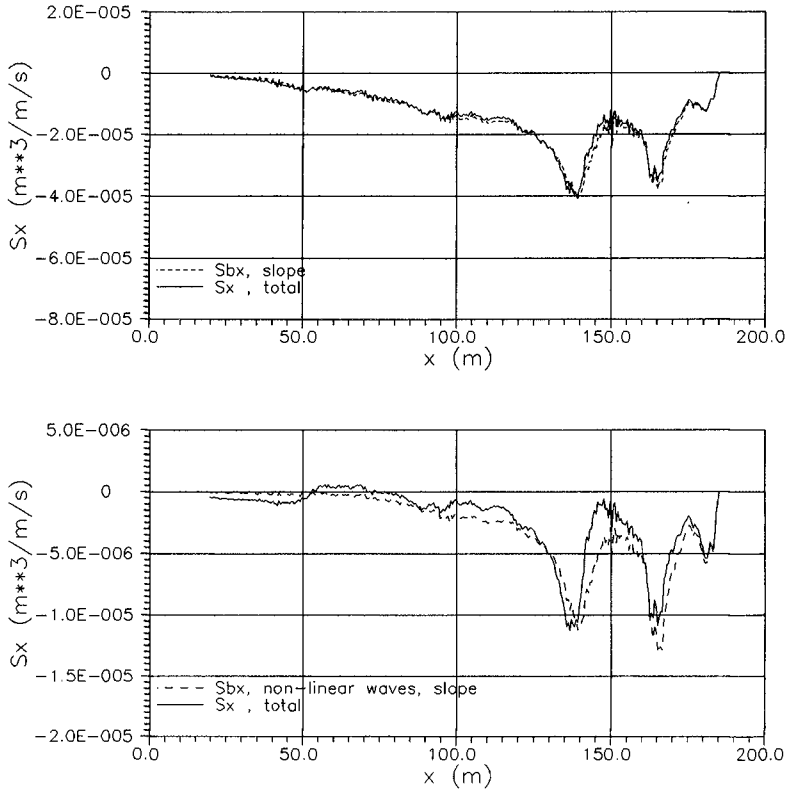


Fig.6 a) Total and bed load (wave-averaged formula),
 b) Total and bed load (interperiod formula with Stokes waves)

transport seems to be captured. The shape can be seen more clearly in Fig. (6b). The interperiod model, although with the wave kinematics rather crudely included, seems to be promising if a new calibration of the van Rijn formula is performed.

Conclusions

A model of cross-shore sediment transport for random waves has been presented. The model consists of the hydrodynamics module, the suspended sediment and the bed load modules. In the suspended sediment module Q-3d velocities and Q-3d concentrations are coupled in a unified formulation while the bed load includes bed slope and wave asymmetry effects.

The behaviour of the hydrodynamic model, in comparison with the Delta Flume data, was rather good. Future improvements would concern correction of the wave model near the shore and the bed shear stress formulation.

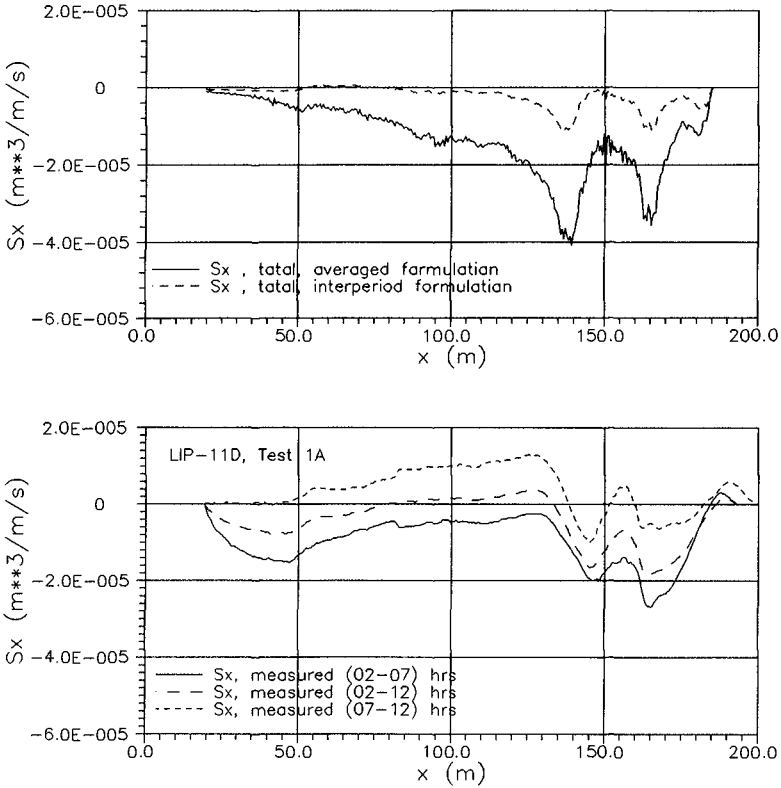


Fig.7 a) Total load (wave-averaged and interperiod formula),
b) Total load (measured)

In the suspended sediment module, the inclusion of the Lagrangian transport was a very important step. The adaptation length for the case examined was very small (and the suspended sediment concentration almost in equilibrium), but this not always the case. The suspended sediment concentrations, although small, should be compared with experimental data.

The wave asymmetry, taken into account in the bed load, was rather conceptually modelled. The wave kinematics should be improved using a suitable wave theory.

The inclusion of the bed slope effect in the bed load is expected to have an important influence on the bed level changes.

The total load was rather good and it is expected to improve as the different modules improve.

Although the model needs certain improvements it has the advantage of integrating most of the components of the cross-shore sediment transport. The swash zone transport, although an important element (see Briand and

Kamphuis, 1993), is not taken into account but before any attempt to include it, the present model has to be improved in the coast line region.

The model should be tested for other dynamic states that would show its capabilities and limitations, starting from tests 1B and 1C of the Delta Flume experiment.

Future research will concern formulation of the model for oblique wave incidence and the coupling of the different modules through the sediment balance equation to yield the bed level evolution.

Acknowledgment

This work was carried out as part of the MAST G8 Coastal Morphodynamics research programme. It was funded by the Commission of European Communities, Directorate General for Science, Research and Development, under MAST contract no. MAS2-CT92-0027.

Appendix I. References

- Battjes, J.A. and Janssen, J.P., 1978.
Energy Loss and Set-up due to Breaking of Random waves, Proc. 16th ICCE, ASCE, pp. 569-588.
- Briand H.M.G. and Kamphuis, J.W., 1993.
Sediment transport in the surf zone: a quasi-3D numerical model. Coastal Engineering, Vol. 20, pp 135-156.
- Fredsøe, J. and Deigaard, R., 1992.
Mechanics of Coastal Sediment Transport. World Scientific, Singapore.
- Galappatti, R. and Vreugdenhil, C.B., 1985.
A depth integrated model for suspended sediment transport. J. Hydr. Res. Vol. 23, No. 4, pp. 359-377.
- De Vriend, H.J. and Stive M.J.F., 1987.
Quasi-3D modelling of nearshore currents. Coastal Engineering, Vol. 11, pp. 565-601.
- Katopodi, I. and Ribberink, J.S., 1992.
Quasi-3D modelling of suspended sediment transport by currents and waves Coastal Engineering, Vol.18, pp. 83-110.
- Katopodi, I., Kitou, N. and de Vriend, H.J., 1992.
Coupling of a quasi-3D model for the transport with a quasi-3D model for the wave induced flow. Proc. 23rd ICCE, Venice, ASCE, pp. 2150-2163.
- Longuet-Higgins, M.S., 1969.
On the transport of mass by time varying ocean currents. Deep Sea Research, Vol. 16, pp. 431-447.
- Ribberink, J.S. and de Vriend, H.J., 1989.
VOORDELTA morphological study, Report H526, Delft Hydraulics.
- Roelvink, J.A. and Brøker, I., 1993
Cross-shore profile models. Coastal Engineering, Vol.21, pp. 163-191.
- S.-Arcilla, A., Roelvink, J.A., O'Connor, B.A. and Himénez, J.A., 1994.
The Delta Flume'93 Experiment. Proc. Coastal Dynamics'93, Barcelona, Spain, ASCE, pp. 488-502.
- Van Rijn, L.C., 1985.
Two-dimensional vertical mathematical model for suspended sediment transport by currents and waves. Delft Hydraulics, Report H461/Q250/Q242
- Van Rijn, L.C., 1986.
Sedimentation of dredged channels by currents and waves. J. of Waterway Port Coastal and Ocean Eng., Vol.112, No.5, pp. 541-559.